

Transmission of low frequency airborne sound in dwellings

By

Francisco Couto

ABSTRACT

The growing importance of the acoustic design of buildings led to the need of developing methods which are able to emulate the sound transmission physics in all frequency range. The normalized methods used for measurement and prediction of sound transmission are not valid at low frequencies due to the modal behavior of sound and vibration fields in this region.

A model for sound transmission of a single wall, based on natural mode analysis, is developed. This method exhibits a good agreement with experimental results. The results highlight the modal behavior of sound transmission at low frequencies.

The method developed in this paper will be used in a parametric analysis to evaluate the error associated with extending the normalized methods to low frequencies and to study the effect of some parameters, such as room dimensions and position of the source or listener, as well as the type of separating wall.

1. INTRODUCTION

Transmission of airborne sound at low frequencies (20 - 200Hz) is a comfort issue in dwellings. As the number of low frequency sound sources used inside and outside dwellings grow, and with the growing demand in comfort as a result of a more mature society, the development of measurement and prediction methods of sound transmission valid also at low frequency becomes even more important.

Even though the average young person is able to understand sounds in the frequency interval from 20Hz to 20000Hz, the current standards used in acoustic designs were conceived to model sound transmission at frequencies in the range 100 - 3150 Hz. The normalized methods used for measurement and prediction of sound transmission are not valid at low frequencies due to the modal behavior, in this region, of the sound and vibration fields.

Thus, this thesis aims to develop a method based on modal analysis that is able to analyze the propagation of airborne sound at low frequencies between two rectangular rooms separated by a plate (see Figure 1). The results of this model will be compared with experimental data obtained by other authors, for validation purposes.

The standard EN12354-1 describes, in its Annex B, a model that allows predictions of airborne sound insulation between rooms in buildings. The method developed in this thesis will be used in a parametric analysis to evaluate the error associated with extending the normalized method to low frequencies and to study the effect of parameters such as room dimensions, position of the sound source or listener.

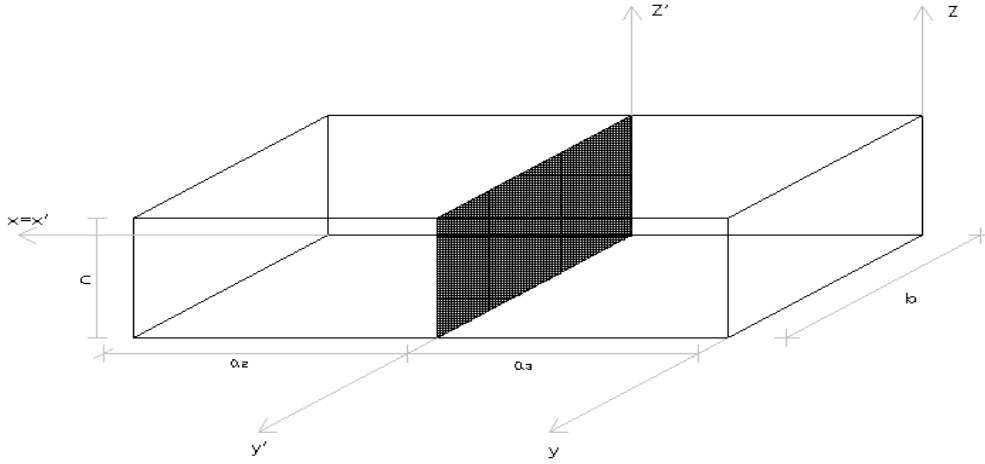


Figure 1 - Rectangular rooms and plate.

2. SOUND FIELD IN THE SOURCE ROOM

The objective of this thesis is to develop a model of airborne sound transmission at low frequencies between two parallelepiped rooms, separated by a wall, using natural mode analysis.

It is, first of all, important to consider a model for the sound field produced in the source room from an airborne source located there. This model considers six hard walls and assumes that the air impedance is much lower than that of the walls.

The pressure in the source room at (x', y', z') from a sound source at (x'_0, y'_0, z'_0) is given by,

$$p(x', y', z') = -j \frac{8Q\omega\rho_0 c_0^2}{a_2 b c} \sum_{l_2, m_2, n_2=0}^{\infty} \left[\frac{\varphi_{l_2 m_2 n_2}(x', y', z') \varphi_{l_2 m_2 n_2}(x'_0, y'_0, z'_0)}{\omega^2 - (\omega_{l_2 m_2 n_2} + j\delta_2)^2} \right]. \quad (1)$$

where:

- $\varphi_{l_2 m_2 n_2}(x', y', z') = \cos\left(\frac{l_2 \pi x'}{a_2}\right) \cos\left(\frac{m_2 \pi y'}{b}\right) \cos\left(\frac{n_2 \pi z'}{c}\right)$, are the mode shape functions of the sound field;

- Q (m^3/s) is the strength of the point source, i.e. the volume velocity with which the point source displaces the surrounding medium;
- ω is the angular frequency of the sound wave (rad/s);
- The eigenfrequencies of the sound field in the source room is given by

$$\omega_{l_2 m_2 n_2} = c_0 \sqrt{\left(\frac{l_2 \pi}{a}\right)^2 + \left(\frac{m_2 \pi}{b}\right)^2 + \left(\frac{n_2 \pi}{c}\right)^2} \text{ (Hz)};$$

- ρ_0 is the static value of the air density, normally estimated by

$$\rho_0 = \frac{P_{atm}}{r_a \theta_K} + \frac{P_w r_a - r_w}{\theta_K r_a r_w};$$

where $r_a = 287 \text{ J.kg}^{-1}\text{K}^{-1}$ and $r_w = 461 \text{ J.kg}^{-1}\text{K}^{-1}$ are the specific gas constants of dry air and water vapor.

- c_0 is the thermodynamic speed of sound given by,

$$c_0 = 331,4 \sqrt{1 + \frac{\theta}{273,15}} \left(\frac{\text{m}}{\text{s}}\right);$$

where θ is the temperature ($^{\circ}\text{C}$);

- δ (s^{-1}) is a temporal absorption coefficient, which is a function of the reverberation time of the room, given by

$$\delta = \frac{6.9}{T_R} = \frac{6.9}{\frac{0,161 V}{A_{eq}}};$$

where the equivalent absorption area of the room (A_{eq} in square meters) is obtained by multiplying the global absorption coefficient of the room (α , assumed to be 0.02) by the area of all room surfaces (S).

This method, was experimentally validated with a considerable degree of accuracy [1]. A point sound source was used in the corner of the test room in order to excite a maximum number of room modes. The sound pressure level was measured in the opposite corner of the room because that is the position in the sound field where the sound pressure level spectrum is known to be more representative of the sound field modes.

Even though the method has the disadvantage of being limited to parallelepiped rooms, this is not a real restriction, since most rooms in dwellings are shoebox shaped. For other shapes, we can use numerical methods, such as the FEM.

Implementation of the model described by equation (1) into a computer program is relatively easy.

3. VIBRATION FIELD

In order to study airborne sound transmission between two parallelepiped rooms, the effect of the vibrating field generated by the separating wall must be considered. Thus, it is necessary to model the vibration of the wall. Assuming that the sound field in the source room is controlled by the sound source only and not by the sound field in the receiving room, which is a valid assumption for heavy walls or high sound levels in the source room, one can consider that the sound field in the receiving room is controlled by the vibration field of the wall that separates the two rooms (see Figure 1).

In this section, the wall is considered homogenous of uniform thickness and simply supported at all edges. Maluski [2] and Neves e Sousa [1] showed that, at low frequencies, this edge conditions approximates reasonably well the real edge conditions.

The transverse velocity field of the wall can be calculated with the model given by Cremer [3], as

$$v_x(y, z) = j \frac{4\omega}{m''bc} \sum_{m_1, n_1=1}^{\infty} \left[\frac{\varphi_{m_1 n_1}(y, z) \int_0^b \int_0^c p(y, z) \varphi_{m_1 n_1}(y, z) dy dz}{\omega_{m_1 n_1}^2 (1 + j\eta) - \omega^2} \right]; \quad (2)$$

With:

- $\varphi_{m_1 n_1}(y, z) = \sin\left(\frac{m_1 \pi y}{b}\right) \sin\left(\frac{n_1 \pi z}{c}\right)$ are the mode shape functions of the vibration field.
- η is the total loss factor. According to the EN ISO 12354, the total loss factor can be approximated by $\eta = (m''/485\sqrt{f}) + 0,01$.
- m'' (kg/m^2) is the mass, which is obtained from the density of the plate material by $m'' = \rho h$ (Kg/m^2), where h is the plate thickness (m).

This method was experimentally validated with a good degree of accuracy for the special case where the excitation is a point force [1].

Implementation of the model described by equation (2) into a computer program is relatively easy. This method has the disadvantage of being limited to rectangular plates, although this shape is current in dwellings.

Equation (2) can now be used together with equation (1) for the sound field in the source room in order to model airborne sound transmission between the two rooms.

4. COUPLING MODEL

In this section, a model for the sound pressure into a room from a vibrating plate-like structure (wall) is presented. This coupling model was developed by Neves e Sousa [1], using natural mode analysis as proposed by Kihlman [4].

The sound field pressure in the receiving room is given by

$$p(x, y, z) = -j\omega\rho_0 \sum_{l_3, m_3, n_3=0}^{\infty} \left[\frac{8C_0^2 (-1)^{l_3} C_{m_3 n_3} \varphi_{l_3 m_3 n_3}(x, y, z)}{a_3 b c \left[(\omega_{l_3 m_3 n_3} + j\delta_3)^2 - \omega^2 \right]} \right], \quad (3)$$

where:

- $\varphi_{l_3 m_3 n_3}(x, y, z) = \cos\left(\frac{l_3 \pi x}{a_2}\right) \cos\left(\frac{m_3 \pi y}{b}\right) \cos\left(\frac{n_3 \pi z}{c}\right)$ are the mode shape functions of the sound field in the receiving room;
- $C_{m_3 n_3}$ are coupling factors given by

$$C_{m_3 n_3} = \int_0^b \int_0^c f(y, z) \cos\left(\frac{m_3 \pi y}{b}\right) \cos\left(\frac{n_3 \pi z}{c}\right) dy dz. \quad (4)$$

as a function of the velocity field $f(y, z) = v_x(y, z)$ of the vibrating plate (separating wall).

Since the coupling factor ($C_{m_3 n_3}$) is known, implementation of equation (3) into a computer program is relatively easy. Neves e Sousa [1] experimentally validated equation (3) for a vibrating field caused by a point force. The results exhibited a good degree of accuracy. Once again, the method has the main disadvantage of being limited to parallelepiped rooms.

Equation (3) will now be used in section 5 along with those for the sound field in the source room and the vibration field of the wall to model the sound field of the receiving room.

5. SOUND FIELD IN THE RECEIVING ROOM

5.1 Model

In this section, a prediction method is developed for the sound field in a room generated by a sound source located in the adjacent room (see Figure 1). This model, just like the previous ones, is derived from natural mode analysis. The model assumes that the sound field in the source room is controlled only by the sound source and room dimensions. It also assumes that the sound field in the receiving room is controlled by the room dimensions and the vibration field of the wall separating the two rooms. Finally, it assumes that the vibration of the wall is controlled only by the sound field in the source room. The method only considers the direct transmission of airborne noise and neglects all types of flanking transmission.

This method is validated with experimental results from Maluski [2].

Assuming that all six walls of the source room are hard walls, the sound pressure at (x', y', z') , caused by a point source with volume velocity Q , located at (x'_0, y'_0, z'_0) , is given by (1). On the other hand, the velocity field induced on a plate due to a pressure field $p(y, z)$ is given by equation (2). Assuming that the pressure field that induces plate vibration results only from the sound pressure generated by the sound source on source room side of the separating wall, according to equation (1), the velocity field of the wall can be calculated by substituting $p(y, z)$ on equation (2) for $p(0, y', z')$, obtained by equation (1), leading to

$$v_x(y, z) = \frac{32Q\omega^2\rho_0c_0^2}{m''a_2b\pi^2} \sum_{m_1, n_1=1}^{\infty} \left\{ \frac{\varphi_{m_1 n_1}(y, z)}{\omega_{m_1 n_1}^2(1 + j\eta) - \omega^2} \sum_{l_2, m_2, n_2=0}^{\infty} \left[\frac{\varphi_{l_2 m_2 n_2}(x'_0, y_0, z_0) \xi_{m_1 n_1 m_2 n_2}}{\omega^2 - (\omega_{l_2 m_2 n_2} + j\delta_2)^2} \right] \right\}, \quad (5)$$

$$\text{Where } \xi_{m_1 n_1 m_2 n_2} = \frac{[(-1)^{m_1+m_2-1}] [(-1)^{n_1+n_2-1}]}{m_1 n_1 \left[\left(\frac{m_2}{m_1} \right)^2 - 1 \right] \left[\left(\frac{n_2}{n_1} \right)^2 - 1 \right]}.$$

Equation (3) can now be used to estimate the sound pressure in the receiving room. Therefore, substituting (5) on (4) and solving the integral for all factors that depend of y or z , yields

$$c_{m_3 n_3} = \frac{32Q\omega^2\rho_0c_0^2}{m''a_2\pi^4} \sum_{m_1, n_1=1}^{\infty} \left\{ \frac{\xi_{m_1 n_1 m_3 n_3}}{\omega_{m_1 n_1}^2(1 + j\eta) - \omega^2} \sum_{l_2, m_2, n_2=0}^{\infty} \left[\frac{\varphi_{l_2 m_2 n_2}(x'_0, y_0, z_0) \xi_{m_1 n_1 m_2 n_2}}{\omega^2 - (\omega_{l_2 m_2 n_2} + j\delta_2)^2} \right] \right\}, \quad (6)$$

$$\text{Where } \xi_{m_1 n_1 m_3 n_3} = \frac{[(-1)^{m_1+m_3-1}] [(-1)^{n_1+n_3-1}]}{m_1 n_1 \left[\left(\frac{m_3}{m_1} \right)^2 - 1 \right] \left[\left(\frac{n_3}{n_1} \right)^2 - 1 \right]}.$$

Finally, substitution of $C_{m_3 n_3}$ from equation (6) into equation (3), gives the sound pressure field in the receiving room as

$$p(x, y, z) = j \frac{256Q\omega^3 \rho_0^2 c_0^4}{m'' a_2 a_3 b c \pi^4} \times \sum_{l_3, m_3, n_3=0}^{\infty} \left[\frac{(-1)^{l_3} \varphi_{l_3 m_3 n_3}(x, y, z)}{(\omega_{l_3 m_3 n_3} + j\delta_3)^2 - \omega^2} \times \dots \right. \\ \left. \dots \times \sum_{m_1, n_1=1}^{\infty} \left\{ \frac{\xi_{m_1 n_1 m_3 n_3}}{\omega_{m_1 n_1}^2 (1 + j\eta) - \omega^2} \sum_{l_2, m_2, n_2=0}^{\infty} \left[\frac{\varphi_{l_2 m_2 n_2}(x'_0, y_0, z_0) \xi_{m_1 n_1 m_2 n_2}}{(\omega_{l_2 m_2 n_2} + j\delta_2)^2 - \omega^2} \right] \right\} \right] \quad (7)$$

Again, implementation of the model described by equation (7) into a computer is relatively easy. First, the room modes are calculated and ordered in a matrix. The plate modes are also calculated and ordered. Then equation (7) is solved. This involves a considerable number of sums. Therefore, the processing time depends greatly on the maximum frequency considered.

5.2 Experimental validation

Experimental validation of this method was done using results obtained by Maluski [2]. Two enclosures of the same dimensions ($1.2 \times 1.2 \times 0.6 \text{ m}^3$) are considered. Two perspex sheets of dimensions $1.43 \times 0.83 \text{ m}^2$ and thickness 10 mm and 5 mm, respectively, formed the party wall. The material properties were assumed as follows: Young's modulus = 5600000000 N/m^2 ; Material density = 1200 kg/m^3 ; Poisson's ratio = 0.4.

The sound source is located at the position $(x'_0, y_0, z_0) = (1.15, 1.15, 0.05) \text{ m}$. The microphone in the source room is located at the position $(x', y', z') = (0.7, 0.8, 0.4) \text{ m}$, and in the receiving room microphone is at the coordinates $(x, y, z) = (0.8, 0.7, 0.4) \text{ m}$.

In order to apply the method described by equation (7), a temperature of $22.5 \text{ }^\circ\text{C}$ is assumed, with a relative humidity of 50%. The strength of the point source was estimated iteratively by successive comparison with experimental results. The total loss factor for the party wall and the global absorption coefficient of the rooms were both assumed as 0.02.

Maluski [2] measured the experimental data between 100 and 800 Hz. Using the method developed in this paper, the frequencies analyzed are from 50 Hz to 800 Hz.

Figure 2 shows the measured and predicted spectrum of sound pressure level obtained with the 5 mm separating plate.

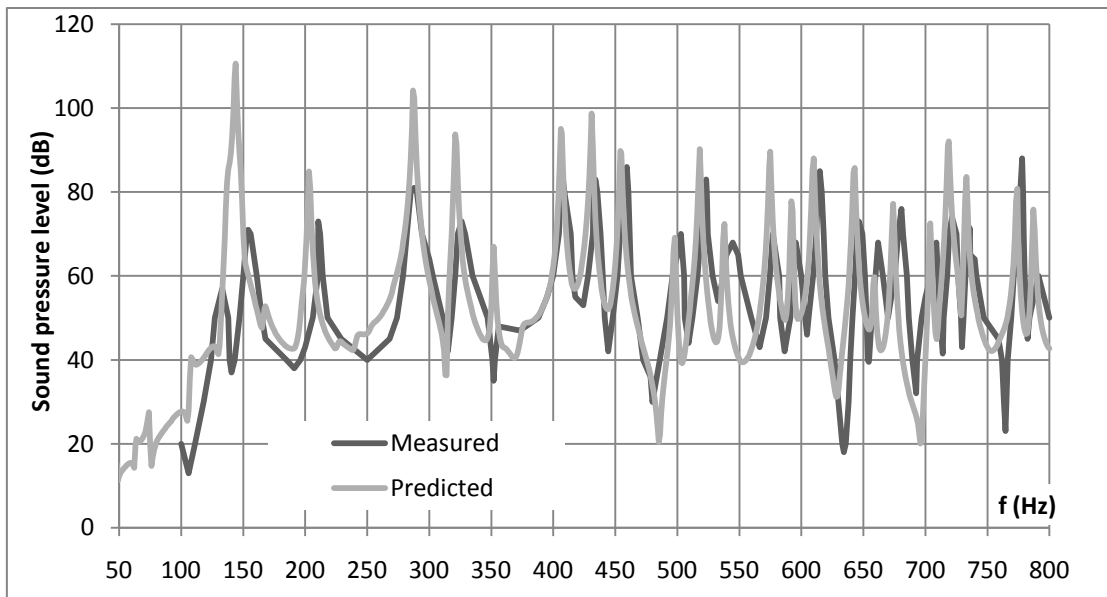


Figure 2 – Measured and predicted frequency response of the 5 mm panel at position $(x,y,z) = (0.8, 0.7, 0.4)$

Figure 3 shows the spectrum of sound pressure level difference obtained with this panel.

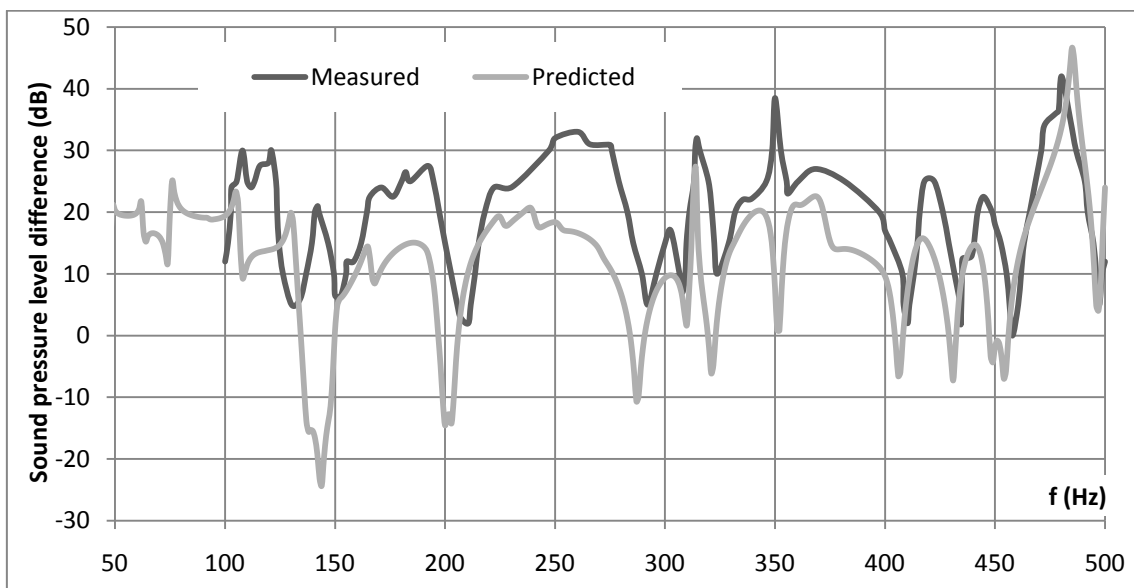


Figure 3 – Sound pressure level difference between position $(x',y',z') = (0.7, 0.8, 0.4)$ of the source room and position $(x,y,z) = (0.8, 0.7, 0.4)$ of the receiving room, for the 5 mm panel.

Figures 2 and 3 highlight the modal behavior of the vibration and sound fields. The most important peaks correspond to the room modes. The vibration field of the plate is only visible at very low frequencies, lower than that corresponding to the first acoustic mode.

Visual inspection shows that there is, in general, a good agreement between the measured and the predicted sound pressure. Equation (7) is therefore experimentally validated. However,

results from equation (7) are, in general, higher than the measured response. This can be minimized by considering a higher temporal absorption coefficient or a lower loss factor of the plate. In practice, imperfections, such as geometrical distortion or structural parameter uncertainty, always exist to a certain extent, which may lead to significant discrepancy from results of theoretical models [5]. This may help to explain the difference between measured and predicted sound pressure levels, particularly for frequencies near the first acoustic mode.

Conclusions are the same for the 5 mm and 10 mm plates.

6. PARAMETRIC ANALYSIS

In this section, the results of a parametric study are discussed. The objective was to identify the effect on airborne sound insulation of factors such as room dimensions, properties of the wall, position of the sound source and sound receptor (listener). 104 cases were analyzed. Each case corresponds to a given configuration of room dimensions, chosen in order to obtain room volumes lower than 50 m³, where low frequency airborne sound insulation is an issue. Only the most important conclusions of such study will be discussed here.

The sound field in the receiving room clearly exhibits a modal behavior. When the sound source and/or the listener are in the centre of the rooms, there are a number of modes which are not excited, thus increasing sound insulation.

As predicted by a number of authors [4,6], airborne sound insulation at low frequencies depends on room dimensions. When the rooms have the same geometry and, consequently, the acoustic modes match, airborne sound insulation is lower. The sound reduction index is generally higher for smaller receiving rooms.

Also the vibration modes of the wall, seem to directly affect airborne sound insulation only at very low frequencies. For higher frequencies, above that corresponding to the first acoustic mode, the vibration modes only affect the amplification obtained at natural acoustic frequencies.

Airborne sound insulation also depends on the type of wall. As expected, for heavier materials such as concrete, a higher airborne sound insulation is obtained in comparison to hollow brick. However, at low frequencies, the wall thickness is comparable to the bending wavelength. For this case, the vibration modes of the plate and coupling to the exciting sound waves have to be taken into account, leading to higher sound insulation with the hollow brick wall at some frequencies.

7. COMPARISON WITH EN 12354-1

The standard EN12354-1 [S.1] describes, in its Annex B, a model for prediction of airborne sound insulation between rooms in buildings for frequencies above 100 Hz. The sound insulation model described in EN 12354-1 [S.1] for the prediction of the sound reduction index does not depend on the room dimensions, sound source and listener positions. It is, therefore, important to understand the error associated with extending the European standard to the low frequency region where the sound field demonstrates a strong modal behavior. The method developed in this thesis can be used to evaluate the precision of the European standard for low frequencies. This was done by using results of the previously described parametric analysis.

The model developed in this thesis was applied to the same wall in several rooms with different lengths (x-dimension). Also the sound source and listener were varied, thus providing a number of index spectra. The lower and upper limits of those spectra are shown in Figure 4 for a concrete wall separating the source room from a receiving room with length varying from 2.90 to 5.70 m. These limits are then compared to the sound reduction index spectrum obtained with the EN 12354-1 [S.1] model.

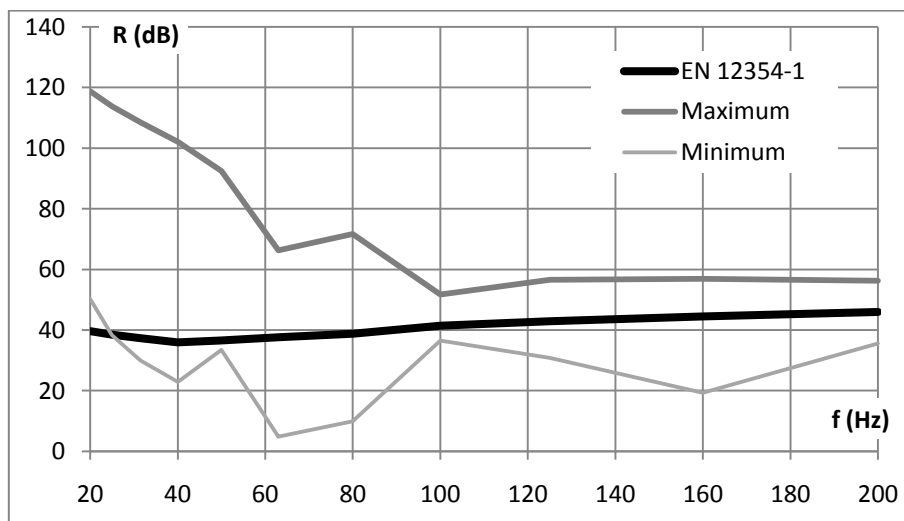


Figure 4 – Sound Reduction index for a general case compared with EN 12354-1 [S.1] results for a concrete wall.

The results of the sound reduction index given in EN 12354-1 [S.1] are, in general, above the lower limit (minimum) obtained analytically. The spread of results is higher for lower frequencies. This shows that there are a number of room configurations yielding lower airborne sound insulation than that predicted by extending the European standard to low frequencies. For frequencies above 100 Hz, the standard method provides more acceptable results.

8. CONCLUSIONS

The normalized prediction method provided by EN 12354-1 [S.1], is based on the classic theories of room acoustics, and therefore it does not take into account the modal behavior of the sound and the vibration fields at low frequencies.

Current standards are therefore unable to describe the sound field at low frequencies. Thus, it is, necessary to develop new sound transmission methods which are valid at low frequencies. The objective of developing and validating such a method, for two parallelepiped rooms separated by a wall, was achieved successfully.

9. REFERENCES

9.1 Books, theses and papers

- [1] Neves e Sousa, A. – Low frequency Impact Sound Transmission in Dwellings, Tese de Doutoramento, The University of Liverpool, 2005;
- [2] Maluski, S. – Low frequencies sound insulation in dwellings; PhD Thesis; University of Sheffield Hallam; United Kingdom;1999;
- [3] Cremer, L.; Hecklo, M.; Ungar, E.E. – Structure-Borne Sound – Structural Vibrations and Sound Radiation at Audio Frequencies – 2nd Edition, Springer-Verlag, Berlin, Germany, 1973;
- [4] Kihlman, T. – Sound radiation into a rectangular room. Applications to airborne sound transmission in buildings, *Acustica*, Vol. 18 (11), pp. 11-20, 1967;
- [5] Li, Y.; Cheng, L. – Vibro-Acoustic Analysis of a rectangular-like cavity with a tilted wall, *Applied Acoustics* 68, pp. 739-751, 2006.
- [6] Donner, U. – Parameterstudien zur Luftschalldämmung kleiner Bauteile, Thesis, Berlin, 1989;

9.2 Standards and regulations

[S.1] EN ISO 12354 – 1 (2000): Building acoustics – Estimation of acoustic performance of buildings from the performance of elements – Annex B: Sound reduction index for monolithic elements.